Spatial and temporal variability of temperature and salinity in the global ocean from Argo float data

*Shigeki Hosoda[1], Kanako Sato[1]

1. Japan Marine-Earth Science and Technology

Statistical analysis for spatial and temporal variability of oceanic temperature and salinity, especially focusing on decorrelation length and signal/noise ratio, is carried out using long-term accumulated Argo float data.
It has been passed 16 years since International Argo program started. The number of active Argo float exceeded 3000 in late 2007, which is the first target in the Argo program, and then the number of accumulated profile data got to 1,000,000 in 2011. As the global Argo observation array is producing real-time oceanic data each horizontally 3x3 degrees every 10 days, we are able to have a huge amount of temperature and salinity data from sea surface to 2000 dbar in the global ocean. The long-term huge Argo data enable us get statistical information of spatial and temporal variability accurately.
Previously such kind of statistical information were estimated for mainly temperature field using eXpendable BathyThermograph (XBT) data (e.g., White, 1995; Meyer et al., 1982). However, sampling area of XBT data is temporally and spatially biased because of limited observational or voluntary ship courses. Recently statistical analyses were carried out using a huge amount of Argo float data to investigate statistical structure of longer term spatial variability on oceanic fields of not only temperature but also salinity. For example, Resnyanskii et al. (2010) showed spatial covariance and signal/noise ratio for separated temperature and salinity fields into 12 areas using Argo data for 2005-2007, and discussed the characteristics of statistical structures depending on areas, temperature/salinity and depth qualitatively. However, they directly analyzed only spatial covariance, indirectly guessed temporal one by global average current velocity.
Using 16-year Argo float data, here we show 4-D statistical structures of accurate decorrelation length and signal/noise ratio, referring the analytical method of Resinyanskii et al. (2010).
Used Argo profiling data are delayed mode quality controlled temperature and salinity in Jan. 2001 - Dec. 2016 obtained from the Argo Global Data Assembly Centers (GDACs) and the Advanced Quality Controlled data (AQC), which is well quality controlled dataset for real-time QC Argo data. Anomalies are calculated from monthly climatology of World Ocean Atlas 2013 (WOA2013: Locarnini et al.,2013; Zweng et al., 2013) to remove seasonal variability. Here we separate the global ocean into 25 areas, which is finer than in the previous study. After sorting all profiling data for each areas, the profiling data are interpolated on 23 levels from 10 to 2000 dbar (Akima, 1970). Then covariance of anomalies are calculated for temperature and salinity fields, sorting into 20km bins of zonal and meridional distances between observations from 0 - 3000km, respectively. Temporal covariance is also calculated from sorted profiling data into 5-day bins from Jan. 2001 to Dec. 2016, referring spatial covariance estimated above. Based on these temporal and spatial covariance maps, we then estimate decorrelation lengths for time, horizontal and vertical directions every areas.
The temporal and spatial covariance exponentially decrease with distances in all area, which are qualitatively similar to the previous study except for temporal covariance that is the first time to analyze in this study. However, some differences of spatial structures on decorrelation length and signal/noise ratio in the previous study are detected in the spatial covariance of temperature and salinity, especially in the difference between temperature and salinity, surface and deeper layers. These results are obtained because of sorting finer area separation into 25 areas and using long-term Argo float data.
The basic statistical information in this study is estimated based only on the purely observational data

from the global Argo array. Therefore, this information is expected to be useful for not only applications for objective analyses and optimal interpolation mapping but also improvement and validation of data assimilation and numerical simulation models.

Keywords: Decorrelation length of oceanic variability, Argo, Global ocean

Long-term change of the halocline in the global ocean

*Oda Masato[1], Ueno Hiromichi[2], Yasui Katsura[1]

1. Graduate School of Environmental Science, Hokkaido University, 2. Faculty of Fisheries Sciences Graduate School of Fisheries Sciences, Hokkaido University

Distribution and long-term change of the halocline in the upper layers of the world ocean were investigated via analysis of World Ocean Database 2013 (WOD13) using a simple definition of the halocline. The halocline was observed in the tropics, equatorward subtropical regions, and subpolar regions, but was absent from central subtropical regions. A strong halocline tended to occur in areas where the sea surface salinity (SSS) was low. Long-term change of the halocline was also observed in the world ocean: halocline was strengthened by more than 20% in the last thirty years in the global average. The change was relatively strong in the tropics, equatorward subtropical regions, and subpolar regions and was closely related with long-term change of SSS: the lower the SSS was, the stronger the halocline became. The correlation coefficient between the horizontal distributions of the halocline strength change and SSS change was -0.55 in the area of 60˚S-60˚N.

Keywords: halocline, long-term change, salinity, global ocean, World Ocean Database

Steric sea level variability from the ocean reanalyses intercomparison project in the East Asian marginal seas

*You-Soon Chang[1], Min-Ji Kang[1]

1. Kongju National University

Ocean Reanalyses Intercomparison Project (ORA-IP) is successfully coordinated, but most analyses using this product have been limited to the global scale assessments. In this study, regional assessment on steric height variability has been performed focusing on the East Asian marginal seas. Results show that reanalysis ensemble derived from 15-different assimilation systems depicts higher correlation with satellite observations (altimetry-gravimetry) than objective analysis ensemble. Additional results about the long-term variability for the thermosteric and halosteric components of each product will be presented.

Keywords: Ocean Reanalyses Intercomparison Project (ORA-IP), steric height, East Asian marginal seas

Diagnosing formation of the severe drought in SWC during 2009-2010

*Lin Feng[1]

1. The First Institute of Oceanography, State Oceanic Administration, China

An extraordinary severe drought hit Southwest China (SWC) from late 2009 to early 2010 and caused enormous losses. The local long-lasting rainfall deficiency which started several months before and the warmer surface air temperature during this period were considered to be the direct meteorological reasons for this disaster. Station observations covering SWC show that there was an almost unbroken rainfall shortage period from May 2009 to March 2010, including two remarkable spells in 2009, May-Jun-July (MJJ) and the boreal autumn (SON). During the first spell, local anomalous descent in the mid-to-low troposphere plays a dominate role to suppress the convection even the water vapor is enough. Diagnosing the vertical motion equation indicates that the local descent is primarily maintained by the anomalous cold temperature advection processes. Both the advection of mean temperature by anomalous wind and the advection of anomalous temperature by mean wind contribute are important. In SON 2009, a quite different situation is proposed that the less than normal northeastward low-level water vapor transport anomaly instead of the descent motions anomaly lead to the rainfall shortage in SWC. Advanced diagnoses illustrate that the low-level water vapor convergence over SWC is significantly less as the transport reduces and the mean water vapor converged by anomalous wind is mainly responsible for this anomaly. Ultimately, the regional circulation anomaly over SWC is controlled by the concurrent El Niño event, which is distinctive and generates an anomalous cyclone centered over the northwest tropical Pacific Ocean.

Keywords: Rainfall , Southwest China, The tropical Pacific

Identification of the Kuroshio and its extension paths from satelite altimeteric measurements.

*Yuya Hirano[1], Kazuyuki Uehara[1]

1. Tokai University

The Kuroshio is the western boundary current of the subtropical gyre of the North Pacific Ocean, it flows eastward along the south coast of Japan. The Kuroshio has typical two paths. One is called large-meander path and the other is called non-large-meander path (Kawabe, 1995).

After the Kuroshio is seperating from east of the Boso penisula, we call the eastward jet as the Kuroshio Extension (KE). It is considered that the KE has basically quasi-stationary meanders with two ridges located at 144 and 150E. Recently, satelite altimetric measurements of the sea surace height field allow us to have been clarified various meander patterns of the KE due to mesoscale eddies and its decadal changes (Qiu and Chen, 2005).

Using sea surface height of satellite altimetric measurements, to determin the path of flows in the ocean is generally very difficult. Determinaion of the KE path, in particular, is difficult because of exisitance of many mesoscale eddies.

In this study, using daily gridded absolute dynamic sea surface height (ADH) distributed by AVISO, we try to determin the paths of the Kurosio/Kuroshi Extension.

Although previous studies have been individually discussed the Kuroshio paths and the KE paths, we here regard the Kuroshio and the KE as one system.

The determination processes of the path are follows. (1) the daily ADH fields and the surface geostrophic flows derived from those are smoothed by 3-month. (2) the maximum absolute geostrophic flows are detected by scanning north-south at the intervals of 1/4 degree longitude from 130E to 140E. The ADHs corresponding the maximum absolute geostrophic flow detected at each longitude are averaged. This mean ADH from 130E to 140E is determined as the ADH which show the Kuroshio path. (3) the start point of the Kuroshio path is determined by the mean ADH on the 126E longitude line. After scanning the south-north along longitude lines and scanning the east-west along latitude lines in order, the next point is selected the shortest distance from among the position of the same values of ADH. (4) this method is repeated to 170E. One path of the Kuroshio/Kuroshio Extension at a instantaneous section is obtained in this way.

We discuss on the statistics of the Kuroshio/Kuroshio Extension paths obtained by the above method.

Keywords: The Kuroshio, The Kuroshio Extension

Internal tides along the Sanriku Coast, Japan

*Kei Nishina[1], Kiyoshi Tanaka[1], Daigo Yanagimoto[1], Hajime Nishigaki[2]

1. Tokyo University, 2. Oita University

Hydrographic observations made in several bays (e.g. Otsuchi bay, Toni bay) on the Sanriku Coast, Japan, detected that baroclinic circulations extending over the bays intermittently occur (e.g. Okazaki, 1990, 1994; Tanaka et al. 2016). Previous studies suggest that the main source of this baroclinic circulation is the internal tides (Okazaki, 1990, 1994; Otobe et al., 1996, 2009; Ito et al., 1998), however, detailed mechanisms are not clear. In the present study, we perform numerical experiments with a two-dimensional (x-z) nonhydrostatic model (Akitomo et al. 1995) in order to investigate the internal tides along the Sanriku Coast focused on the amplification process of the baroclinic circulation over the bays. Experimental results (Figure 1) indicate that the internal waves enhance the baroclinic circulations over the bays. This internal waves are generated at the shelf break and propagate to the bay mouth.

Keywords: internal tide, Sanriku, shelf-break, nonhydrostatic model

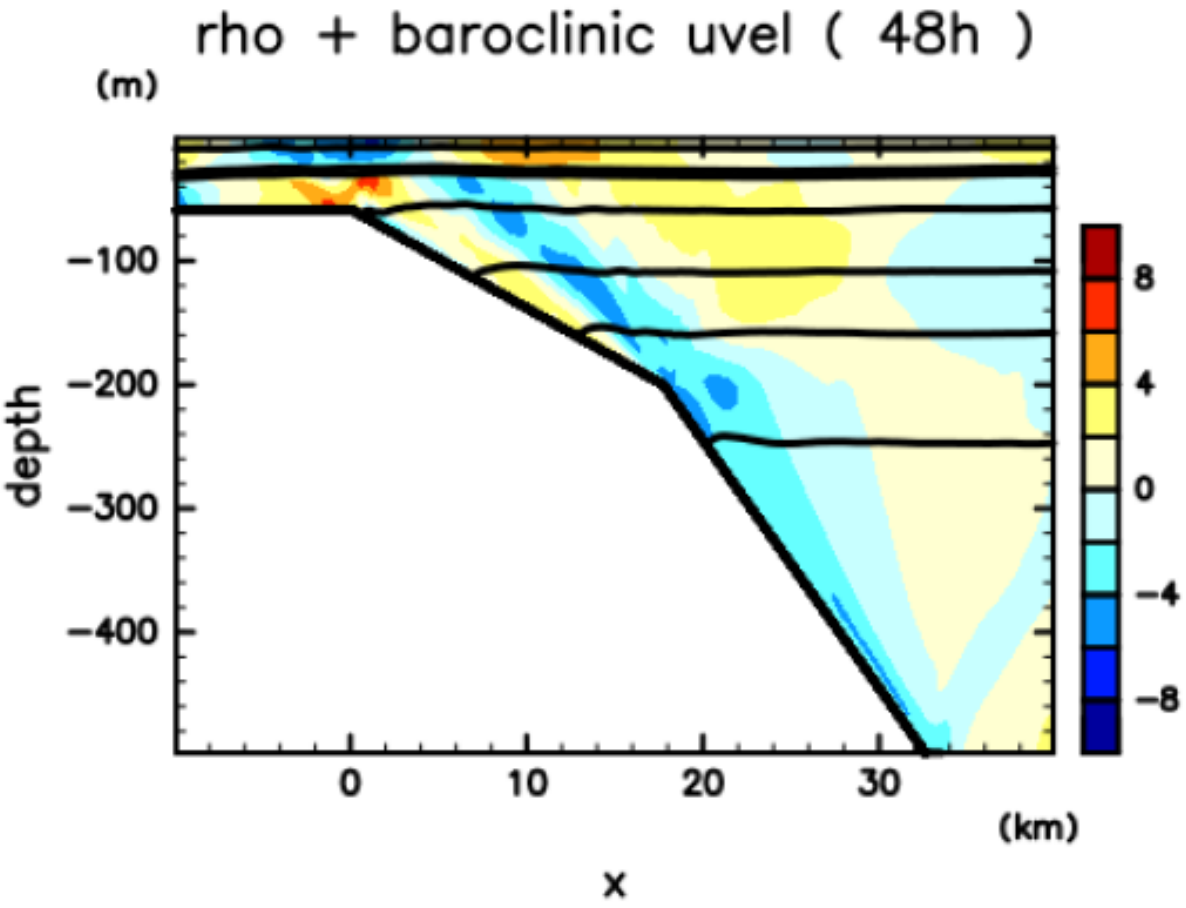

Figure 1. Experimental results of baroclinic cross-shore velocity (color tone, cm/s) and potential density (contour, contour interval 0.5 kg m^{-3})

